Continuous wave ridge waveguide lasers in femtosecond laser micromachined ion irradiated Nd:YAG single crystals

Yuechen Jia,[1] Ningning Dong,[1] Feng Chen,[1,*] Javier R. Vázquez de Aldana,[2] Shavkat Akhmadaliev,[3] and Shengqiang Zhou[3]

[1]*School of Physics, Key Laboratory of Particle Physics and Particle Irradiation (MOE) and State Key Laboratory of Crystal Materials, Shandong University, Jinan 250100, China*
[2]*Laser Microprocessing Group, Universidad de Salamanca, Salamanca 37008, Spain*
[3]*Institute of Ion Beam and Materials Research, Helmholtz-Zentrum Dresden- Rossendorf, Dresden 01314, Germany*
**drfchen@sdu.edu.cn*

Abstract: Ridge waveguides have been fabricated in Nd:YAG single crystal by using femtosecond laser micromachining in an oxygen ion irradiated planar waveguide. The microphotoluminescence features have been found well preserved in the waveguide structures. Continuous wave lasers have been realized at 1.06 μm at room temperature in the ridge waveguide system with a lasing threshold of ~39 mW and a slope efficiency of 35%, which show superior performance to the planar waveguide.

OCIS codes: (230.7370) Waveguides; (140.3390) Laser materials processing; (130.3120) Integrated optics devices.

References and links

1. C. Grivas, "Optically pumped planar waveguide lasers, Part I: Fundamentals and fabrication techniques," Prog. Quantum Electron. **35**(6), 159–239 (2011).
2. F. Chen, "Construction of two-dimensional waveguides in insulating optical materials by means of ion beam implantation for photonic applications: Fabrication methods and research progress," Crit. Rev. Solid State Mater. Sci. **33**(3-4), 165–182 (2008).
3. P. D. Townsend, P. J. Chandler, and L. Zhang, *Optical Effects of Ion Implantation* (Cambridge Univ. Press, Cambridge, UK, 1994).
4. F. Chen, "Micro-and submicrometric waveguiding structures in optical crystals produced by ion beams for photonic applications," Laser Photon. Rev. DOI: 10.1002/lpor.201100037.
5. M. Domenech, G. V. Vázquez, E. Cantelar, and G. Lifante, "Continuous-wave laser action at λ= 1064.3 nm in proton- and carbon- implanted Nd:YAG waveguides," Appl. Phys. Lett. **83**(20), 4110–4112 (2003).
6. E. Flores-Romero, G. V. Vázquez, H. Márquez, R. Rangel-Rojo, J. Rickards, and R. Trejo-Luna, "Planar waveguide lasers by proton implantation in Nd:YAG crystals," Opt. Express **12**(10), 2264–2269 (2004).
7. Y. Y. Ren, N. N. Dong, F. Chen, A. Benayas, D. Jaque, F. Qiu, and T. Narusawa, "Swift heavy-ion irradiated active waveguides in Nd:YAG crystals: fabrication and laser generation," Opt. Lett. **35**(19), 3276–3278 (2010).
8. Y. Y. Ren, N. N. Dong, F. Chen, and D. Jaque, "Swift nitrogen ion irradiated waveguide lasers in Nd:YAG crystal," Opt. Express **19**(6), 5522–5527 (2011).
9. Y. C. Yao, Y. Tan, N. N. Dong, F. Chen, and A. A. Bettiol, "Continuous wave Nd:YAG channel waveguide laser produced by focused proton beam writing," Opt. Express **18**(24), 24516–24521 (2010).
10. A. G. Okhrimchuk, A. V. Shestakov, I. Khrushchev, and J. Mitchell, "Depressed cladding, buried waveguide laser formed in a YAG:Nd^{3+} crystal by femtosecond laser writing," Opt. Lett. **30**(17), 2248–2250 (2005).
11. G. A. Torchia, A. Rodenas, A. Benayas, E. Cantelar, L. Roso, and D. Jaque, "Highly efficient laser action in femtosecond-written Nd:yttrium aluminum garnet ceramic waveguides," Appl. Phys. Lett. **92**(11), 111103 (2008).
12. J. Siebenmorgen, K. Petermann, G. Huber, K. Rademaker, S. Nolte, and A. Tünnermann, "Femtosecond laser written stress-induced Nd:$Y_3Al_5O_{12}$(Nd:YAG) channel waveguide laser," Appl. Phys. B **97**(2), 251–255 (2009).
13. T. Calmano, J. Siebenmorgen, O. Hellmig, K. Petermann, and G. Huber, "Nd:YAG waveguide laser with 1.3W output power, fabricated by direct femtosecond laser writing," Appl. Phys. B **100**(1), 131–135 (2010).
14. J. Olivares, A. García-Navarro, A. Méndez, F. Agulló-López, G. García, A. García-Cabañes, and M. Carrascosa, "Novel optical waveguides by in-depth controlled electronic damage with swift ions," Nucl. Instrum. Methods Phys. Res. B **257**(1-2), 765–770 (2007).
15. A. García-Navarro, J. Olivares, G. García, F. Agulló-López, S. García-Blanco, C. Merchant, and J. S. Aitchison, "Fabrication of optical waveguides in KGW by swift heavy ion beam irradiation," Nucl. Instrum. Methods Phys. Res. B **249**(1-2), 177–180 (2006).

#165357 - $15.00 USD Received 23 Mar 2012; revised 11 Apr 2012; accepted 17 Apr 2012; published 18 Apr 2012

16. P. Kumar, S. Moorthy Babu, S. Ganesamoorthy, A. K. Karnal, and D. Kanjilal, "Influence of swift ions and proton implantation on the formation of optical waveguides in lithium niobate," J. Appl. Phys. **102**(8), 084905 (2007).
17. Y. Y. Ren, N. N. Dong, Y. C. Jia, L. L. Pang, Z. G. Wang, Q. M. Lu, and F. Chen, "Efficient laser emissions at 1.06 μm of swift heavy ion irradiated Nd:YCOB waveguides," Opt. Lett. **36**(23), 4521–4523 (2011).
18. F. Chen, "Photonic guiding structures in lithium niobate crystals produced by energetic ion beams," J. Appl. Phys. **106**(8), 081101 (2009).
19. S. Juodkazis, V. Mizeikis, and H. Misawa, "Three-dimensional microfabrication of materials by femtosecond lasers for photonics applications," J. Appl. Phys. **106**(5), 051101 (2009).
20. R. R. Gattass and E. Mazur, "Femtosecond laser micromachining in transparent materials," Nat. Photonics **2**(4), 219–225 (2008).
21. M. Ams, G. D. Marshall, P. Dekker, J. Piper, and M. Withford, "Ultrafast laser written active devices," Laser Photon. Rev. **3**(6), 535–544 (2009).
22. R. Degl'Innocenti, S. Reidt, A. Guarino, D. Rezzonico, G. Poberaj, and P. Günter, "Micromachining of ridge optical waveguides on top of He^+-implanted β-BaB_2O_4 crystals by femtosecond laser ablation," J. Appl. Phys. **100**(11), 113121 (2006).
23. Z. F. Bi, L. Wang, X. H. Liu, S. M. Zhang, M. M. Dong, Q. Z. Zhao, X. L. Wu, and K. M. Wang, "Optical waveguides in TiO_2 formed by He ion implantation," Opt. Express **20**(6), 6712–6719 (2012).
24. A. Ródenas, G. A. Torchia, G. Lifante, E. Cantelar, J. Lamela, F. Jaque, L. Roso, and D. Jaque, "Refractive index change mechanisms in femtosecond laser written ceramic Nd:YAG waveguides: micro-spectroscopy experiments and beam propagation calculations," Appl. Phys. B **95**(1), 85–96 (2009).
25. A. Ródenas, D. Jaque, C. Molpeceres, S. Lauzurica, J. L. Ocaña, G. A. Torchia, and F. Agulló-Rueda, "Ultraviolet nanosecond laser-assisted micro-modifications in lithium niobate monitored by Nd^{3+} luminescence," Appl. Phys., A Mater. Sci. Process. **87**(1), 87–90 (2007).
26. R. Ramponi, R. Osellame, and M. Marangoni, "Two straightforward methods for the measurement of optical losses in planar waveguides," Rev. Sci. Instrum. **73**(3), 1117–1120 (2002).
27. H. Sun, F. He, Z. Zhou, Y. Cheng, Z. Xu, K. Sugioka, and K. Midorikawa, "Fabrication of microfluidic optical waveguides on glass chips with femtosecond laser pulses," Opt. Lett. **32**(11), 1536–1538 (2007).
28. J. F. Ziegler, computer code, SRIM, *http://www.srim.org*.

1. Introduction

Waveguide lasers based on active media are the minor light sources that play important roles in integrated photonics and modern telecommunication systems owing to their compact dimensions [1]. The mode volume is strongly compressed in the active waveguides, leading to high optical intensities of pump beams inside the structures and thus, in an optimized condition, the lasing threshold is lower than that of the bulks, and the slope efficiency could be optimized comparable to the bulk lasers [1]. Compared with one-dimensional (1D) (planar or slab waveguides), the two-dimensional (2D) (in channel or ridge configurations) waveguides can confine the light propagation in 2Ds, reaching higher optical density, and are possible to construct more compact devices [2].

Neodymium doped yttrium aluminum garnet (Nd:$Y_3Al_5O_{12}$ or Nd:YAG) crystal is one of the most favorable gain media for solid state lasers owing to its excellent fluorescence, physical and thermal properties. Waveguide lasers have been realized in Nd:YAG crystals in the systems manufactured by ion beam implantation/irradiation [3–9] or femtosecond laser inscription [10–13]. Recently, the irradiation of swift heavy ions (i.e., with energy higher than 1 MeV/amu) has emerged to be a powerful and available technique to fabricate optical waveguide owing to the reduced irradiation fluences and larger refractive index changes for waveguide formation [4,14]. Compared to the normal light ion implantation, in which case the refractive index changes leading to the formation of waveguides are mainly given by the nuclear damage contribution [4,14–18], the refractive index modification mainly happens during most path of the incident ions' trajectory via the impact of amorphous or highly defective nanotracks from a single ion or the overlap of a few ions. In recent works, Ar and N ions was utilized to fabricated planar waveguides in Nd:YAG crystal for waveguide lasers by using swift heavy ion irradiation technique [7,8]. Nevertheless, a ridge structure is necessary and advantageous for more compact lateral confinement of light fields. The femtosecond (fs) laser ablation technique has become increasingly attractive in recent years owing to the various practical applications in microstructuring of numerous materials [19–21]. In fact, the fs laser ablation has been successfully applied to fabricate ridge waveguide structures on the surface of $LiNbO_3$, β-BaB_2O_4 and TiO_2 planar waveguides [18,22,23]. In this work, we report on the construction of ridge waveguide in Nd:YAG crystals by combining swift oxygen ion

#165357 - $15.00 USD Received 23 Mar 2012; revised 11 Apr 2012; accepted 17 Apr 2012; published 18 Apr 2012

irradiation and fs laser ablation, and the realization of continuous wave (cw) waveguide lasers at wavelength of 1.06 μm.

2. Experiments in details

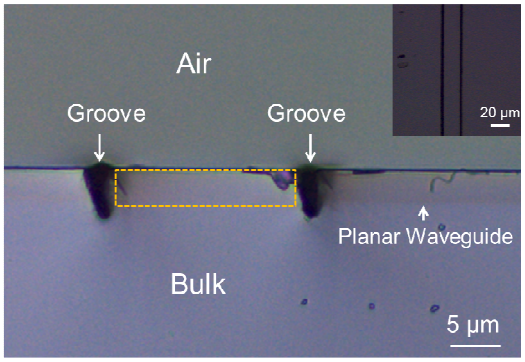

Fig. 1. Optical microscope image of the end face of the ridge waveguide (dashed line surrounded region) fabricated by the fs laser ablated 17 MeV O^{5+} ion irradiated Nd:YAG crystal. The inset shows the top view of the ridge waveguide.

The Nd:YAG crystal (doped by 2 at. % Nd^{3+} ion) used in this work was cut to dimensions of 10 × 5 × 2 mm^3 and optically polished. One sample surface (10 × 5 mm^2) was irradiated with the oxygen (O^{5+}) ions at energy of 17 MeV and fluence of 2 × 10^{14} ions/cm^2 by using the 3MV tandem accelerator at Helmholtz-Zentrum Dresden-Rossendorf, Germany, to form a planar waveguide layer. The ion current density was kept at a low level (around 6-8 nA/cm^2) to avoid the heating and charging of the sample. And then, on top of the irradiated surface (i.e., the planar waveguide surface), we used a Ti:Sapphire laser system (Spitfire, Spectra Physics), which delivers nearly transform-limited pulses with a temporal duration of 120 fs and a central wavelength of 796 nm (spectral width: 9 nm) and with a repetition rate of 1 kHz, to micromachine the ridge structures. The laser beam was focused by a 20 × microscope objective (N.A. = 0.4), and the sample was located at a XYZ motorized stage with a spatial resolution of 0.2 μm. The focus of the convex was located on the irradiated surface of the sample and the pulse energy was set to 2.1 μJ (peak fluence ~50 J/cm^2). The sample was scanned at a translation velocity of 50 μm/s, as a compromise between having a moderate processing time and obtaining the crater depth enough to equal the depth of the planar waveguide layer. At this translation velocity, the mean number of incident pulses reaching each point of the sample is ~35, producing a crater depth of ~5 μm. Then, pairs of grooves were fabricated with lateral separation of 20 μm. With the lateral confinement of microstructured grooves and vertical restriction of ion irradiated planar waveguide, the ridge waveguide was produced in Nd:YAG crystal with a length of 10 mm. Figure 1 shows the microscope image of the cross section of the ridge waveguide. For comparison, about 1/3 of the surface layer is not microstructured, preserving the planar waveguide geometry.

The confocal micro-photoluminescence (μ-PL) properties of the 17 MeV O^{5+} ion irradiated planar waveguide were measured by an Olympus BX-41 fiber-coupled confocal microscope equipped with an argon laser. The laser radiation at 488 nm was focused onto the samples by using a 100 × objective with numerical aperture N.A. = 0.95, exciting the transition of Nd^{3+} ions through $^4I_{9/2} \rightarrow {}^2G_{3/2}$ [24,25]. Then, the subsequent $^4F_{3/2} \rightarrow {}^4I_{9/2}$, $^4I_{11/2}$ emission generated from Nd^{3+} ions was collected by using the same microscope objective and, after passing through a confocal aperture, analyzed by a CCD camera attached to a high resolution fiber-coupled spectrometer. The sample was mounted on an XY motorized stage with a spatial resolution of 100 nm to scan the 488 nm excitation spot over the waveguide's cross section.

We measured the propagation losses of the planar and ridge waveguides by using the back-reflection method [26]. The propagation losses for the planar and ridge waveguide were

#165357 - $15.00 USD Received 23 Mar 2012; revised 11 Apr 2012; accepted 17 Apr 2012; published 18 Apr 2012

~2.5 and 3.8 dB/cm at 632.8 nm, respectively. The higher attenuation for ridge waveguide should be partly attributed to the non-perfect side-walls fabricated by the fs lasers. The roughness of the side walls was estimated to be ~1 μm by the SEM image. One can expect the reduction of the roughness of the side walls by either using ion beam milling [22] or multi-scan (instead of single-scan) of fs laser ablation [27], which will reduce the propagation losses further. The Fresnel reflection loss was ~0.8 dB at the interface between the waveguide and the air. The coupling loss of the ridge waveguide system was ~12 dB.

The waveguide laser operation experiment was performed by utilizing a typical end-face pumping system. A polarized light beam at 808 nm generated from a tunable cw Ti:Sapphire laser (Coherent MBR 110) was used as the pump source. A convex lens with focal length of 25 mm focused the pump laser beam into the planar waveguide. An input mirror (with the transmittance of 98% at 808 nm and the reflectivity >99% at ~1064 nm) and an output mirror (with the reflectivity >99% at 808 nm and transmittance of 60% at ~1064 nm) were adhered to the two end facets of the Nd:YAG waveguide, forming a Fabry-Perot lasing resonate cavity. The generated waveguide laser was collected by utilizing a 20 × microscope objective lens (N.A. = 0.4) and imaged by using an infrared CCD camera. We used a spectrometer with resolution of 0.2 nm to record the emission spectra of the waveguide lasers.

3. Results and discussion

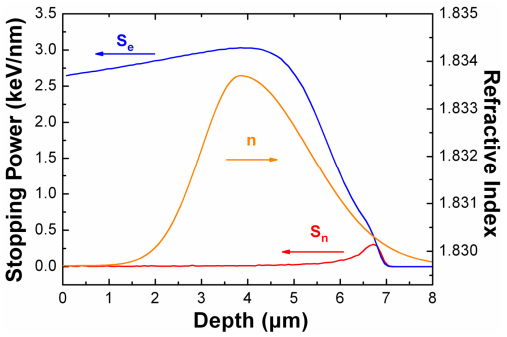

Fig. 2. The S_e (blue line), S_n (red line) curves as well as the refractive profile of the waveguide (yellow line) as a function of the depth from the sample surface.

We calculated the profiles of the nuclear (S_n) and electronic (S_e) stopping powers of incident 17 MeV O^{5+} ions in Nd:YAG crystals by utilizing the SRIM 2010 code [28], as shown in Fig. 2. As one can see, nonvanishing values of S_e are obtained within the first 0-7 μm, peaking at about 3 keV/nm at a depth of ~4μm, completely overwhelming those of S_n, which are about zero within the range of 0-4 μm and climbs to the maximum value of approximately 0.3 keV/nm at around 6.7 μm beneath the surface of the sample. Similar to the early reported swift Ar or N ion irradiated Nd:YAG waveguides [7,8], it is reasonable to consider that the O ion irradiated waveguide is also mainly induced by electronic damage created lattice changes of the Nd:YAG matrix.

The change of the refractive index (Δn) of the waveguide layer was estimated by measuring the maximum incident angle Θ_m of the planar waveguide at which no change of the transmitted power is occurring, and the maximum refractive index increase was calculated to be $\Delta n \approx + 0.004$ by using the formula

$$\Delta n = \frac{\sin^2 \Theta_m}{2n} \tag{1}$$

where Θ_m is the maximum incident angular deflection at which no transmitted power change is occurring, while $n = 1.8297$ is the refractive index of the unmodified substrate [12]. By combination of this refractive index change with the S_e profile, we have reconstructed the refractive index distribution of the planar waveguide (as shown in Fig. 2).

#165357 - $15.00 USD Received 23 Mar 2012; revised 11 Apr 2012; accepted 17 Apr 2012; published 18 Apr 2012

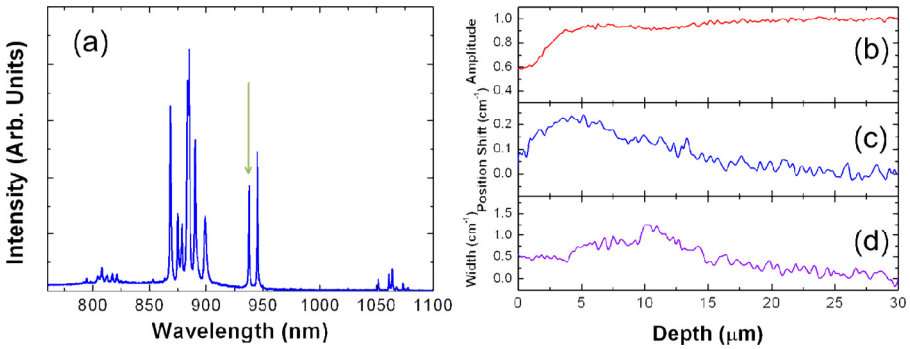

Fig. 3. (a) Typical luminescence spectrum of $^4F_{3/2}\rightarrow{}^4I_{9/2}$ and $^4F_{3/2}\rightarrow{}^4I_{11/2}$ transition of Nd ions in the bulk Nd:YAG crystal. 1D spatial scan of the emitted intensity (b), spectral shift (c) and spectral broadening (d) of the hyper-sensitive 937.8 nm Nd^{3+} emission line.

Figure 3(a) shows the typical luminescence spectrum ($^4F_{3/2}\rightarrow{}^4I_{9/2}$ and $^4F_{3/2}\rightarrow{}^4I_{11/2}$ transitions of Nd^{3+} ions) of the bulk of Nd:YAG crystal. For detailed understanding of the modification of the O^{5+} ions on the PL properties in the waveguides, we focused on this hyper-sensitive 937.8 nm emission line (marked by an arrow in Fig. 3(a)). Figures 3(b), 3(c) and 3(d) depict the 1D μ-PL profiles based on the spectral intensity, spectral shift and spectral broadening of this line, respectively. As we can see, the intensity has a reduction from the sample surface to the depth of ~7 μm. The minimum is around 60% of the amplitude of the bulk. The fluorescence intensity reduction is mainly attributed to lattice damage (lattice defects and imperfections etc.) induced by the electronic damage during the O^{5+} ions irradiation process, and one can conclude that this result is in good agreement with the electronic stopping power profile as shown in Fig. 2. However, in the waveguide core region (i.e., at the depth of 4μm), the PL intensity of 90% of the bulk has been preserved, which means that the waveguide region is still very active. The position shift profile denotes that the emission line has been shifted to larger energies along the whole ion trajectory with a peak at the depth of ~4 μm, where the S_e is maximized. The maximum value of the blue shift is 0.25 cm^{-1}. In addition, the maximum for the spectral broadening is 1.25 cm^{-1}. The remarkable line broadening is due to the presence of lattice disorder along the ion trajectory.

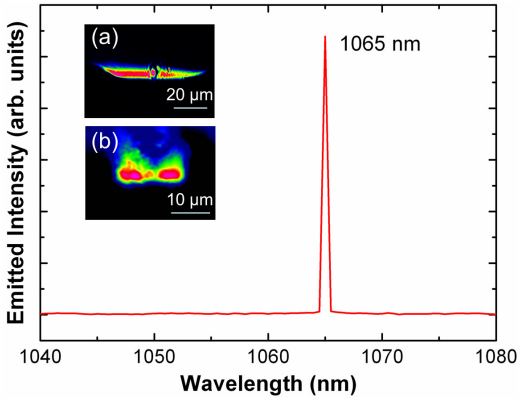

Fig. 4. Laser emission spectrum from the planar and ridge Nd:YAG waveguides. The insets show the measured near-field intensity distribution of the (a) planar and (b) ridge waveguide laser modes.

Figure 4 depicts the laser emission spectra from 17 MeV O^{5+} ion irradiated Nd:YAG planar and ridge waveguide. The center wavelength of the laser emission from the waveguides is 1065 nm, clearly denoting laser oscillation line that corresponds to the main fluorescence of $^4F_{3/2}\rightarrow{}^4I_{11/2}$ transition of Nd^{3+} ions.

#165357 - $15.00 USD Received 23 Mar 2012; revised 11 Apr 2012; accepted 17 Apr 2012; published 18 Apr 2012

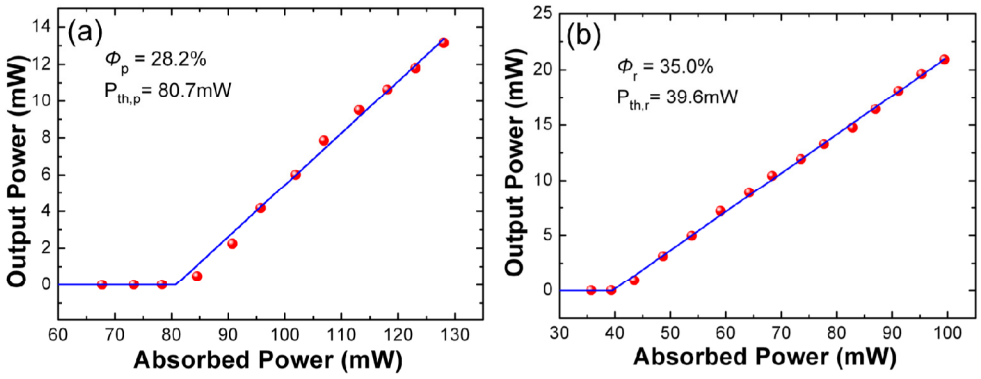

Fig. 5. Output laser power at 1065 nm as a function of absorbed pump power at 808 nm obtained from the Nd:YAG (a) planar and (b) ridge waveguide.

Figures 5(a) and 5(b) show the output laser powers (at wavelength of 1065 nm) as a function of the 808 nm absorbed powers generated in the Nd:YAG planar and ridge waveguide at room temperature. From the linear fit of the experimental data, we have determined that the lasing thresholds for the 1065 nm oscillations are $P_{th,p}$ = 80.7 mW and $P_{th,r}$ = 39.6 mW for the planar and ridge waveguides, respectively. And the slope efficiencies are Φ_p = 28.2% and Φ_r = 35%, respectively. As the absorbed pump power increases, the output laser power of these two waveguides climbed to maxima at $P_{max,p}$ = 13 mW and $P_{max,r}$ = 21 mW at absorbed pump powers of 128 mW and 100 mW, respectively. Compared with the Nd:YAG planar waveguide, the ridge waveguide system possesses a superior performance with reduced lasing threshold, higher slope efficiency and higher output laser power. These results indicate that the Nd:YAG ridge waveguide produced by fs-laser micromachining of planar waveguide layer could be a promising candidate for compact light sources.

4. Summary

We have reported on the optical ridge waveguide in Nd:YAG laser crystals fabricated by using 17 MeV O^{5+} ion irradiation and fs laser ablation technique. The waveguide was formed in the electronic damage region, which confined laterally by two fs laser grooves. The μ-PL properties have been well preserved in the waveguides, suggesting lattice disorder happened within the ion trajectory. The stable cw waveguide laser at 1065 nm was realized with the lasing threshold of 39.6 mW and the slope efficiency of 35%. By comparison, the Nd:YAG ridge waveguide shows a superior laser performance to the planar one. This work also suggests that the technique with combination of ion irradiation and fs laser ablation may be an efficient method to fabricate ridge waveguides in a large range of optical materials.

Acknowledgments

The work is supported by the National Natural Science Foundation of China (No. 10925524), the Spanish Ministerio de Ciencia e Innovación (MICINN) through Consolider Program SAUUL CSD2007-00013 and Project FIS2009-09522. S.Z. acknowledges the funding by the Helmholtz-Gemeinschaft Deutscher Forschungszentren (HGF-VH-NG-713). Support from the Centro de Láseres Pulsados (CLPU) is also acknowledged.

#165357 - $15.00 USD Received 23 Mar 2012; revised 11 Apr 2012; accepted 17 Apr 2012; published 18 Apr 2012